The Effect of a C-Terminal Peptide of Surfactant Protein B (SP-B) on Oriented Lipid Bilayers, Characterized by Solid-State ^{2}H- and ^{31}P-NMR

Tran-Chin Yang,[†] Mark McDonald,[‡] Michael R. Morrow,[‡] and Valerie Booth[†‡*]
[†]Department of Biochemistry, and [‡]Department of Physics and Physical Oceanography, Memorial University of Newfoundland, St. John's, Canada

ABSTRACT SP-B_{CTERM}, a cationic, helical peptide based on the essential lung surfactant protein B (SP-B), retains a significant fraction of the function of the full-length protein. Solid-state ^{2}H- and ^{31}P-NMR were used to examine the effects of SP-B_{CTERM} on mechanically oriented lipid bilayer samples. SP-B_{CTERM} modified the multilayer structure of bilayers composed of POPC, POPG, POPC/POPG, or bovine lipid extract surfactant (BLES), even at relatively low peptide concentrations. The ^{31}P spectra of BLES, which contains ~1% SP-B, and POPC/POPG with 1% SP-B_{CTERM}, look very similar, supporting a similarity in lipid interactions of SP-B_{CTERM} and its parent protein, full-length SP-B. In the model systems, although the peptide interacted with both the oriented and unoriented fractions of the lipids, it interacted differently with the two fractions, as demonstrated by differences in lipid headgroup structure induced by the peptide. On the other hand, although SP-B_{CTERM} induced similar disruptions in overall bilayer orientation in BLES, there was no evidence of lipid headgroup conformational changes in either the oriented or the unoriented fractions of the BLES samples. Notably, in the model lipid systems the peptide did not induce the formation of small, rapidly tumbling lipid structures, such as micelles, or of hexagonal phases, the observation of which would have provided support for functional mechanisms involving peptide-induced lipid flip-flop or stabilization of curved lipid structures, respectively.

INTRODUCTION

Lung surfactant (LS) is a mixture of lipids and proteins that is essential for reducing surface tension at the air-aqueous interface during breathing (1,2). It is secreted from alveolar type II cells and transferred into the aqueous layer lining the alveoli, where it forms a surface monolayer with underlying multilayer structures (3). Approximately 90% by weight of surfactant is lipid, mainly phosphocholine (PC) and phosphoglycerol (PG), and 10% is surfactant proteins (SPs) (4,5). To date, four proteins, designated by their chronologic order of discovery as SP-A, SP-B, SP-C, and SP-D, have been identified. Proteins SP-A and SP-D are large, hydrophilic oligomers that possess activities against bacteria or viruses and thus provide important host defense functions (4,6–8). Although SP-A can affect surfactant lipid organization, it plays less critical roles in surface activity than the small hydrophobic proteins SP-B and SP-C, whereas SP-D has no known surface activity at all (9). Both SP-B and SP-C promote adsorption and spreading of phospholipids into the air-aqueous interface (3,10), and also influence the organization and readsorption of the multilayer structures thought to be important as reservoirs during inspiration/expiration cycling (11). Of all the LS proteins, SP-B leads to the largest reductions in surface tensions (12) and is the only LS protein that is essential for life (4,13,14).

SP-B is highly conserved in mammalian species (6) and possesses 79 amino acid residues per monomer. Six cysteines form three intramolecular disulfide bonds, and the seventh one forms an intermolecular bridge to stabilize the SP-B homodimer structure (15,16). SP-B contains a predominantly α-helical conformation as determined by circular dichroism and Fourier transform infrared spectroscopy (17,18). High-resolution structures of several subsegments of SP-B have been determined by solution NMR spectroscopy: these include an N-terminal SP-B (SP-$B_{11–25}$) peptide in methanol solution (19), the C-terminus of SP-B (SP-$B_{63–78}$) in hexafluoro-2-propanol organic solvent and sodium dodecyl sulfate (SDS) micelles (20), and Mini-B, a 34-residue peptide containing both N- and C-terminal regions of SP-B, in SDS micelles (21). All of these peptides display a high proportion of amphipathic α-helix conformation. Several fragments of SP-B containing one or more of its helices have been shown to retain a significant portion of the function of full-length SP-B in in vitro and in vivo studies (22–26). SP-$B_{63–78}$ retains almost half the activity of full-length SP-B, as judged by in vivo studies in surfactant deficient rats (26) (A. Waring and F. Walther, University of California, Los Angeles, personal communication, 2007).

The C-terminal peptide, SP-$B_{63–78}$ or SP-B_{CTERM}, employed in this study has 16 residues with a net charge of +3 as compared to the full-length protein, which has a charge of +7 (per monomer) at neutral pH. It has been suggested that the function of SP-B is related to its positive charges and amphipathic helical structure (27,28). The C-terminal region of SP-B formed a basis for the design of the 21-residue peptide KL4 (29), which has shown promise as a synthetic replacement for SP-B in clinical trials (30,31).

Although it is thought that SP-B plays critical roles in accelerating or stabilizing the formation of surface active monolayer films, a detailed mechanistic understanding of all the complex interactions between the lipid and protein components that

Submitted July 24, 2008, and accepted for publication February 3, 2009.

*Correspondence: vbooth@mun.ca

Editor: Marc Baldus.

0006-3495/09/05/3762/10 $2.00

doi: 10.1016/j.bpj.2009.02.027

underlie LS function has not yet been established. In the lung, LS is found both in monolayer structures at the air/water interface and in the multilayer structures that are closely associated with the interfacial monolayer. Although many mechanisms for SP-B have been proposed, several center around its potential role in promoting the organization of the lipids into specific, functional structures (32,33). For example, SP-B has been proposed to hold hypophase multilayer structures in close association with the surface monolayer by interacting with both structures (32). It has also been hypothesized that SP-B might promote fusion of the multilayer structures with the monolayer by stabilizing negatively curved lipid structures in the neck region of the fusion structure (11). Additionally, there have been some suggestions that SPs, including SP-B, may promote lipid adsorption to the surface by inducing flip-flop of lipids (34,35). In this study, SP-B_{CTERM}'s ability to manipulate multilayer structures was probed by monitoring the peptide-induced changes in NMR spectra of mechanically aligned lipid bilayers. Unlike multilamellar dispersions, oriented bilayers provide information on large-scale lipid organization, as well as on lipid acyl chain order and headgroup orientation in both the oriented and peptide-disrupted fractions of the sample. In addition to revealing SP-B_{CTERM}'s effect on the overall lipid organization, the NMR spectra would have indicated the formation of any hexagonal phase material. Such an observation would support a role for the peptide in inducing highly curved bilayer structures such as those seen in fusion-neck regions, or the presence of rapidly reorienting species that could support a role for SP-B in inducing lipid flip-flop (34,35).

Although LS is composed of a complex mix of lipids, two-component mixtures composed of a ratio of 7:3 PC/PG have been shown to successfully mimic many of the characteristic of LS (36,37), and have been used in artificial surfactant (ALEC) (38,39). The saturated lipid dipalmitoylphosphatidylcholine (DPPC) is generally considered to be of paramount importance in attaining low surface tensions, although, for example, in bovine LS, the amounts of DPPC and unsaturated PC are approximately equal (11), and there are some organisms with functioning LS that contain quite low levels of DPPC (40). In this study, it was deemed more advantageous to employ POPC rather than DPPC in the model lipid systems to focus on the effects of headgroup composition and to avoid complications due to the high liquid crystal phase to gel phase transition temperature of DPPC, and consequent difficulties with maintaining sample hydration. Our study employed a mixture of 7:3 1-palmitoyl-2-oleoyl-*sn*-glycero-3-phosphocholine (POPC) to 1-palmitoyl-2-oleoyl-*sn*-glycero-3-phosphoglycerol (POPG), as well as POPC alone and POPG alone. The work was extended to include DPPC, as well as most other components of LS, by repeating the experiments with bovine lipid extract surfactant (BLES), which is prepared from endotracheal lavage of cow lungs (41). BLES is an LS that is used clinically and contains all the normal components of LS, except for cholesterol and other neutral lipids, as well as the hydrophilic LS proteins SP-A and SP-D, which are removed.

MATERIALS AND METHODS

Materials

SP-B_{CTERM} (NH_2-GRMLPQLVCRLVLRCS-COOH), a peptide consisting of residues 63–78 of human SP-B, was synthesized via solid phase methods employing *O*-fluorenylmethyl-oxycarbonyl (Fmoc) chemistry, and purified using HPLC as previously described (20). POPC, POPC-d_{31}, POPG, and POPG-d_{31} were purchased from Avanti Polar Lipids (Alabaster, AL) and used as received. BLES was a gift from BLES Biochemicals (London, Canada) and was used after an additional $CH_3OH/CHCl_3$ extraction based on Bligh and Dyer methods (42), with concentration determined by UV absorption at 815 nm. Muscovite mica (grade V-4, dimension: 75 × 25 × 0.26 mm^3) was purchased from Structure Probe (West Chester, PA) and cut into smaller pieces with dimension 12.5 mm × 5 mm and thickness of ~40 μm.

Preparation of oriented samples

Peptide and 4 mg of lipids or BLES were codissolved in a solvent composed of $CH_3OH/CHCl_3$ (1:1 by volume), without buffer or salt. The secondary structure of the peptide in this solution is α-helical, as confirmed by circular dichroism (see Fig. S1 in the Supporting Material). In all samples except for those containing BLES, 30% (by weight) of the lipids were deuterated, i.e., 7:3 POPC/POPC-d_{31}, 7:3 POPG/POPG-d_{31}, or 7:3 POPC/POPG-d_{31}. The ^2H and ^{31}P spectra for each particular peptide/lipid (P/L) composition were obtained with exactly the same sample. The concentration of P/L is expressed in percentage, based on their weights. The solution, with a total volume of ~250 μL, was spread homogeneously with care on 12 mica plates. The unstacked plates were dried for ~2 h in a fume hood and then placed in a vacuum chamber overnight. Each plate was then spread with several microliters of double-distilled water and put in a hydration chamber with saturated ammonia phosphate solution at 4°C for at least 3 days. The plates were then stacked together, wrapped with plastic film, and sealed with polystyrene plastic. Samples were stored at 4°C before and after use. Since double-distilled water rather than deuterium-depleted water was used to hydrate the samples, the ^2H-NMR signal contribution from double-distilled water was examined and found to be negligible compared to the signal from ^2H-labeled lipid (<30 times the intensity of the CD_3 peak; data not shown). Several samples were subjected to thin film chromatography and the lipids showed a single spot (data not shown), indicating that the bilayer orientation disruption observed was not the result of lipid hydrolysis.

NMR experiments

The spectra were acquired on a Bruker (Billerica, MA) Avance II 14.1 Tesla solid-state NMR spectrometer at a temperature of 293 K and operated at resonance frequencies of 243.02 MHz and 92.15 MHz for nuclei ^{31}P and ^2H, respectively. Except where noted, each spectrum was acquired with the bilayer normal parallel to the external magnetic field, using the average of 8192–10,240 transients with spectral line-broadening of 100 Hz applied during processing. For ^{31}P experiments, the sample was inserted into a Bruker dual-tuned cross-polarization flat coil probe. A spin-echo pulse sequence ($\pi/2$-τ-π-acq) was applied, with a $\pi/2$ pulse length of 12 μs, a delay τ of 2 μs, and a recycle delay of 3 s. The spectral width was 184 ppm, with SPINAL-64 proton decoupling at a strength of 60 kHz (43). The chemical shift was externally referenced to 85% H_3PO_4 as 0 ppm. It has been shown that for oriented samples such as these, with <100 mg of mica, the chemical shift deviation due to the nonspherical geometry of the sample is <1 ppm (44). For ^2H experiments, the sample was inserted into a Bruker triple-tuned cross-polarization flat coil probe. A quadrupole echo pulse sequence ($\pi/2$-τ-$\pi/2$-acq) (45) was used with $\pi/2$ and τ set at 2.5 μs and 15 μs, respectively. The spectral width was 200 kHz, with a recycle delay of 1 s.

Deuterium peak assignment and order parameter determination

To examine the effect of the peptide on orientational order at different points along the POPC lipid chain, the peaks in the ^{2}H-NMR spectra were assigned to the appropriate carbon positions along the (*sn*1) acyl chain. The innermost pair is assigned to the methyl group (C16) deuterons at the tail end of the lipids, which have the least constrained motion. The pair with the second smallest splitting is assigned to deuterons (on C15) next to the methyl group, and so on for deuterons on C14 and C13. In the region of the spectra with wider splittings (the plateau region), the doublets overlap. For these resonances, the dependence of orientational order on position can be estimated using the smoothed order parameter profile approach (46). In this approach, the peak positions are estimated by dividing the area of the spectrum corresponding to deuterons on C12 to C2 into 11 equal parts and assuming that the quadrupole splitting changes monotonically with position along the chain.

Note that both of these assignment approaches could be applied even to most of the ^{2}H spectra that exhibited contributions from unoriented lipid components. Although the unoriented fraction of the sample contributed some broad intensity to the central region, the C16-C13 peaks from the oriented portion of the sample could be clearly identified for all but the POPG/peptide samples. Since the unoriented portion of the sample does not contribute to the intensity in the wider (plateau) region of the spectra, the smoothed order parameter approach could still be applied for C12-C2.

Using the deuteron assignment scheme described above, the order parameter of the lipid chains was probed at different positions along the chains. For the oriented bilayer spectral component, the quadrupole splitting $\Delta\nu_{CD}{}^{i}$ of deuterons on a lipid acyl chain at the *i*-th carbon position is given by

$$\Delta\nu_{CD}^{i} = \frac{3\nu_{CD}}{2}\left|S_{CD}^{i}\right|, \quad (1)$$

where ν_{CD} is the quadrupole coupling constant of deuterium, given by 167 kHz in deuterated paraffin hydrocarbons (47), and S_{CD}^{i} is the C-D bond order parameter in the *i*-th segment. It can be expressed as

$$S_{CD}^{i} = \left\langle 3Cos^2\theta^i - 1\right\rangle/2, \quad (2)$$

where θ^i is the angle between the C-D bond of the *i*-th segment and the bilayer normal, and the brackets indicate the time ensemble average.

The mean-torque model developed by Petrache et al. (48) was used to quantify the average area, $\langle A\rangle$, per lipid (*sn*1) chain and the average hydrocarbon thickness D_C per monolayer. For this, only the average S_{CD}^{i} at carbon positions 2–6 was used.

RESULTS

SP-B_{CTERM} in pure POPC lipids

First, the effects of SP-B_{CTERM} on oriented bilayers composed of pure POPC were investigated by acquiring ^{2}H-NMR spectra of oriented samples with varying peptide contents (Fig. 1 *a*). In the absence of peptide, the peaks are well resolved and show that the lipid bilayers are well aligned. As peptide is added, the quadrupole splitting is observed to decrease and the spectra become superpositions of more than one component, one component with larger splittings, corresponding to bilayers oriented with bilayer normal parallel to the magnetic field and a second component having features with splittings that are half of the oriented component splittings (see *arrows* in Fig. 1 *a*). The second component is most likely due to randomly oriented bilayers. Isotropically reorienting structures such as micelles would give rise to an unsplit feature of significant intensity at 0 kHz. The spectra in Fig. 1 *a* suggest that any fraction of isotropic material present in these samples must be very small.

^{31}P spectra of the same samples were acquired to obtain further insight into the effect of the peptide on both the oriented and unoriented components of the samples (Fig. 1 *b*). In the absence of peptide, the ^{31}P spectra exhibit a single peak at 34.2 ppm, corresponding to the $\sigma_{//}$ peak. The signal intensity in the spectral region spanning 0 and −20 ppm is negligible, confirming that the lipid bilayers are well aligned with their normals parallel to the external magnetic field. When peptide at a concentration of 5% (w/w) is present in the POPC sample, the chemical shift of the $\sigma_{//}$ peak does not change appreciably, but the intensity at $\sigma_{//}$ decreases and a weak, broad peak centered at ~−12 ppm appears. When the concentration of peptide in the sample is increased to 10%, the intensity of $\sigma_{//}$ is further decreased and the frequency is shifted downfield to 38.0 ppm. In other words, at 10% concentration the presence of the peptide affects the conformation of the lipid headgroups in the portion of the POPC sample that remains oriented.

For phosphatidylcholine and phosphatidylglycerol, which have isotropic chemical shift close to 0 ppm (49), the

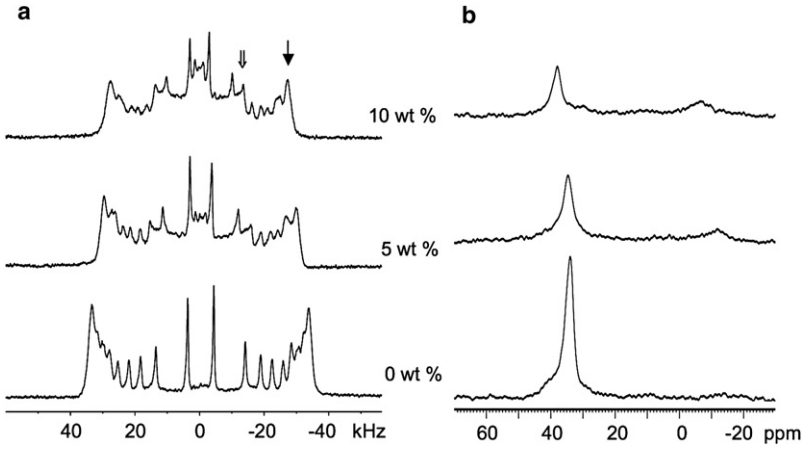

FIGURE 1 ^{2}H- (*a*) and ^{31}P- (*b*) NMR spectra for POPC (POPC/POPC-d_{31} = 7/3, w/w) in the presence of increasing concentrations of SP-B_{CTERM}, where "→" and "⇒" indicate oriented and randomly orientated species, respectively. The external magnetic field ($\mathbf{B_0}$) is parallel to bilayer normal ($\mathbf{n}$); $\mathbf{B_0}$ // $\mathbf{n}$.

unoriented lipid material would be expected to contribute significant intensity to the spectrum at $\sigma_\perp \approx -\sigma_{//} / 2$, the chemical shift for bilayers oriented with their normal perpendicular to the external field. Hence, if the lipid headgroup orientation were the same in the oriented and unoriented fractions of the samples, we would expect the peaks deriving from the unoriented lipids to appear at −17.1 and −19.0 ppm for 5% and 10% peptide, respectively. What is observed, however, are peaks at −12 ppm for 5% peptide and −6 ppm for 10% peptide, and so it appears that the peptide induces a different lipid headgroup conformation in the unoriented portion of the sample as compared to the oriented lipids. This difference in conformation is slight at 5% but more pronounced at 10% peptide. On the other hand, the ^{2}H splittings of the oriented fraction are double the splittings of the unoriented fraction (Fig. 1 *a*) to within the precision with which such splittings can be determined. That is to say, even though the headgroup conformation is different in the oriented and unoriented fractions of the sample, the acyl chains in the oriented and unoriented fractions have the same orientational order characteristics.

SP-B_{CTERM} in pure POPG lipid

The quadrupole splittings in the ^{2}H spectra of POPG (Fig. 2 *a*) are smaller than those for POPC, indicating that the motion of lipid acyl chains in POPG is less restricted. This presumably reflects the effect of electrostatic repulsion of the charged POPG headgroups on the average area per lipid. Similarly to POPC, as peptide is added to the POPG bilayers the quadrupole splittings decrease and a second spectral component with half the splittings, due to randomly oriented material, appears. In contrast to POPC, the peaks in the POPG + peptide spectra broaden significantly and become less resolved. This may reflect a peptide-induced broadening of the distribution of bilayer normal orientations about the direction of the magnetic field, a contribution from the effects of strong peptide-lipid interactions on relaxation time, or a combination of both effects (50).

Fig. 2 *b* shows the corresponding ^{31}P spectra for POPG. The inclusion of 5% peptide causes a downfield shift of the $\sigma_{//}$ peak from 31.4 ppm to 32.0 ppm, as well as a reduction in this peak's intensity, along with the appearance of a new peak at ~−4 ppm. The peptide's effect on POPG is stronger than its effect on POPC, as judged by the greater changes in ^{31}P $\sigma_{//}$ peak chemical shift and intensity for POPG, as well as on the fraction of unoriented material and line-broadening evident in the ^{2}H spectra. The larger effect of the peptide on the anionic POPG as compared to the zwitterionic POPC is not unexpected given the peptide's charge of +3.

The wings at the base of the ^{31}P $\sigma_{//}$ peak with 5% peptide (Fig. 2 *b*) support the conclusion that at least some of the line-broadening observed in the ^{2}H spectra is due to mosiac spread of the bilayer stack. Although the new peak at ~−4 ppm induced by the presence of 5% peptide is close to the isotropic chemical shift, $\sigma_{iso} \approx 0$ ppm, the ^{2}H spectrum indicates no isotropically reorienting species, and thus the −4 ppm peak can be attributed instead to randomly oriented lipids. This $\sigma_\perp$ peak appears significantly downfield of the chemical shift expected based on the $\sigma_{//}$ peak (−4 ppm vs. $\sigma_\perp = -\sigma_{//} / 2 = -15.7$ ppm), which indicates that although the peptide interacts with both the oriented and unoriented fractions of the lipids, it does not induce the same headgroup conformation in each phase. The splittings of the ^{2}H spectra (Fig. 2 *a*) scale as expected at 5% peptide, with the oriented material displaying splittings at twice the unoriented splitting. However, at 10% peptide, the splittings of the oriented lipids are noticeably smaller than twice the unoriented splittings, indicating that the peptide has a differential effect on the lipid chains in the oriented and unoriented fractions of the lipids.

At 10% peptide, the ^{31}P spectrum changes greatly in character (Fig. 2 *b*) with two upfield peaks at 8.8 and −10.5 ppm. This type of pattern was observed in ^{31}P spectra of lipids in the presence of antimicrobial peptides and attributed to hexagonal phase material (51,52). However, this possibility can be ruled out by the ^{2}H spectrum (Fig. 2 *a*), which displays no evidence of material with splittings at ~1/4 the oriented

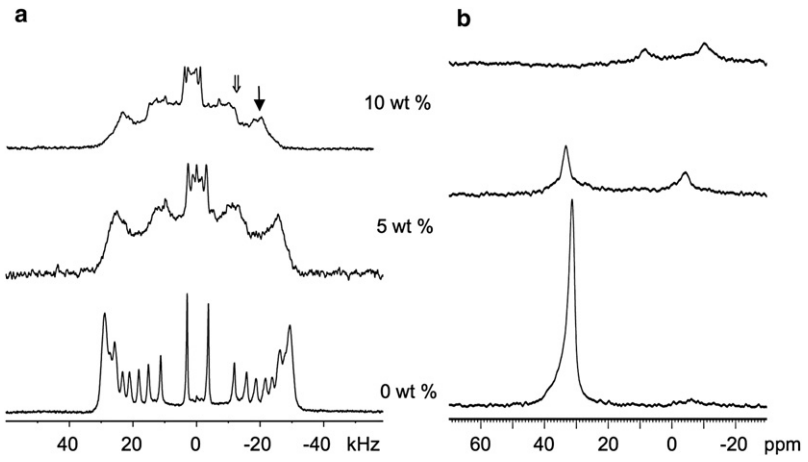

FIGURE 2 ^{2}H- (*a*) and ^{31}P- (*b*) NMR spectra (at $\mathbf{B_0}$ // **n**) for POPG (POPG/POPG-d_{31} = 7/3, w/w) in the presence of increasing concentrations of SP-B_{CTERM}, where "→" and "⇒" indicate oriented and randomly orientated species, respectively.

sample splitting that would correspond to hexagonal material with cylindrical axes oriented parallel to the bilayer surface. Although a hexagonal phase with cylindrical axes oriented perpendicular to the bilayer surface would have intensity at 1/2 the oriented sample splitting, it is hard to imagine how this would form without some cylinders aligned parallel to the surface of the oriented layers. Instead, the −10.5 ppm ^{31}P peak likely represents randomly oriented lipids, and the peak at 8.8 ppm could indicate a population of oriented lipids with a large peptide-induced change in average headgroup orientation relative to the bilayer normal. A change from 32 to 8.8 ppm would correspond to a change in average headgroup tilt of ~45° (49), which is well within the broad distribution of tilt angles observed in simulations of PC bilayers (53,54) but is quite large; therefore, headgroup tilt may not explain this shift in peak position. A large change in headgroup tilt is supported by the decrease in chain order indicated by the reduction in maximum ^{2}H splitting with 10% SP-B_{CTERM}. The strong perturbation of the headgroups likely generates a relatively wide distribution of headgroup orientations and therefore weakens the maximum intensity of the ^{31}P peaks, as observed.

SP-B_{CTERM} in 7:3 POPC/POPG mixed lipid bilayers

In the next step of this work, we employed bilayers composed of 7:3 POPC/POPG-d_{31} to characterize the effect of the peptide on a model system with a headgroup composition that is commonly used in LS research. In the absence of peptide, the ^{2}H peaks are well resolved, indicating well-aligned bilayers (Fig. 3 *a*). Again, addition of the peptide appears to broaden the spectral features associated with the oriented bilayer component, and to introduce a second spectral component with features at half the splitting of the corresponding oriented spectral features. The second component is again attributed to peptide-induced disruption of the bilayer orientation and the resulting formation of unoriented bilayer material. Unlike in pure POPG, even at 10% peptide, the splitting of the oriented component is close to double the splitting of the powder component, indicating that the perturbation of the POPG-d_{31} chains by SP-B_{CTERM} is roughly equivalent in the oriented and powder components of the sample.

In the absence of SP-B_{CTERM}, the ^{31}P spectrum (Fig. 3 *b*) indicates well-aligned lipid bilayers. The $\sigma_{//}$ frequencies are at ~36.7 ppm (for POPC) and 32.4 ppm (for POPG), with an intensity ratio close to the 7/3 value expected given the lipid composition of the sample. At high concentrations of peptide (i.e., 2.5–10%), the $\sigma_{//}$ peak of POPG-d_{31} is shifted upfield by ~5 ppm to ~27 ppm, with a much smaller upfield shift in the $\sigma_{//}$ peak of POPC. Similarly to the single lipid studies, addition of peptide to the POPC/POPG-d_{31} mixture leads to a decrease in the intensity of the $\sigma_{//}$ peaks and a concomitant appearance of intensity in the upfield portion of the spectra. However, the effect of the peptide on the POPG-d_{31} ^{31}P peak intensity in the POPC/POPG-d_{31} mixed samples (Fig. 3 *b*) is much smaller than its effect on the POPG spectra in the sample with POPG alone (Fig. 2 *b*), as judged by the position and intensity of the $\sigma_{//}$ peak. A comparison of the area under the deconvoluted $\sigma_{//}$ peak (not shown) in the POPC/POPG-d_{31} ^{31}P spectra to the areas in the single lipid samples indicates that the presence of POPG increases the effect of the peptide on the POPC, and the presence of POPC decreases the effect of the peptide on the POPG. For example, the ratio of areas for aligned PC, at the $\sigma_{//}$ frequency, in Fig. 3 *b* (POPC/POPG/peptide$_{10\%}$: POPC/POPG/peptide$_{0\%}$) and Fig. 1 *b* (POPC/peptide$_{10\%}$: POPC/peptide$_{0\%}$) is 0.3 (±0.1) and 0.4 (±0.1), respectively, indicating that the POPC is more perturbed by the peptide in the presence of 30% POPG than when POPC is the only lipid present.

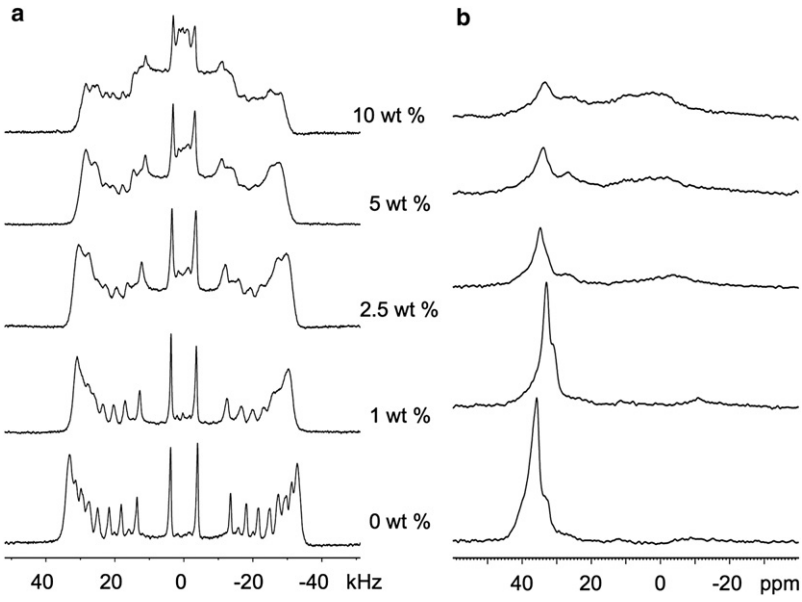

FIGURE 3 ^{2}H- (*a*) and ^{31}P- (*b*) NMR spectra (at $\mathbf{B_0}$ // $\mathbf{n}$) for mixed lipids POPC/POPG-d_{31} (= 7/3, w/w) in the presence of increasing concentrations of SP-B_{CTERM}.

In the POPC/POPG-d_{31} mixed lipid samples, the new modes of lipid organization brought about by the presence of SP-B_{CTERM} give rise to a broad peak centered at ~−12 ppm at 1% peptide, but shifting toward 0 ppm at 5% and 10% peptide. Although intensity at 0 ppm could reflect a population of isotropically reorienting material, this possibility is eliminated by the ^{2}H spectra, and thus it likely reflects randomly oriented material with a peptide-induced change in headgroup conformation. The $\sigma_\perp$ peak is broader in POPC/POPG-d_{31} than in either of the single-lipid samples, indicating a larger range of headgroup orientations in the unoriented fraction of the mixed lipid sample. It is also centered more downfield than either of the single lipid samples, indicating a different average headgroup angle.

SP-B_{CTERM} in BLES

Finally, the effect of SP-B_{CTERM} on a near-complete LS was probed with the use of BLES. The BLES samples were analyzed by ^{31}P-NMR because ^{31}P is the naturally occurring isotope. Deuterium NMR studies were not done, since such studies would have involved perturbing the system by the addition of ^{2}H-labeled lipids.

In Fig. 4, the ^{31}P spectra show the effect of SP-B_{CTERM} on oriented BLES. In the absence of peptide, the lipids in BLES can be almost as well aligned as those in the POPC/POPG sample, and the PC and PG peaks can be resolved. However, unlike the POPC/POPG sample with 0% peptide, in BLES a broad peak occurs at ~−11 ppm even in the absence of peptide. This small percentage of unaligned material is likely due to the effect of the natural SP-B in the BLES, which is ~1% of the total surfactant (41). Indeed, the spectrum of BLES with no additional peptide is very similar to the spectrum of POPC/POPG with 1% peptide (Fig. 3 *b*). Addition of SP-B_{CTERM} to the BLES leads to a significant increase in the amount of randomly oriented material, with the $\sigma_{//}$ peak becoming indistinguishable at 7.5%. The appearance of the ^{31}P spectrum at 7.5% peptide is very close to a purely powder pattern spectrum, as expected for unoriented lipids, with just a small amount of extra intensity remaining at ~32 ppm, indicating a small amount of residual orientation. In contrast to the POPC/POPG samples, the new peaks observed upon addition of the peptide do not appear near 0 ppm. Instead, they appear significantly upfield of this, at ~−11 ppm, which is close to the $\sigma_\perp$ frequency of POPC and POPG. There is also no discernible shift in the $\sigma_{//}$ peak from 0 to 2.5% peptide. Thus it appears that addition of SP-B_{CTERM} to BLES leads to loss of bilayer orientation, but with no change of lipid headgroup conformation in either the oriented or unoriented fractions of the sample.

DISCUSSION

SP-B_{CTERM} disrupted the orientation of the mechanically aligned bilayers in all of the systems studied, as demonstrated by the attenuation of the $\sigma_{//}$ ^{31}P peak with peptide addition (Figs. 1 *b*, 2 *b*, 3 *b*, and 4, and Fig. S2 a). Such behavior is likely related to SP-B's ability to promote fusion of monolayers and bilayers, which must involve some sort of disruption to the regular multilayer structure. On the other hand, SP-B_{CTERM} did not induce the formation of small, rapidly tumbling lipid structures, such as micelles, the observation of which might lend support to a role for SP-B in promoting insertion of the lipids into the air/water interface by inducing lipid flip-flop transitions. Additionally, SP-B_{CTERM} did not induce formation of hexagonal phases, the observation of which might support a role for SP-B in promoting lipid insertion by stabilizing negatively curved lipid structures. It should be noted, however, that the absence of such phenomena in the fluid lipid phases employed in this study does not necessarily mean they are not possible in the highly compressed lipid phases present in the lungs upon expiration.

Like SP-B_{CTERM}, full-length SP-B has an overall positive charge, which has led others to examine the potential preference of SP-B for anionic lipids. No consensus has yet been reached; in some studies a preference for DPPG over DPPC was observed (55,56), whereas in others SP-B appeared to

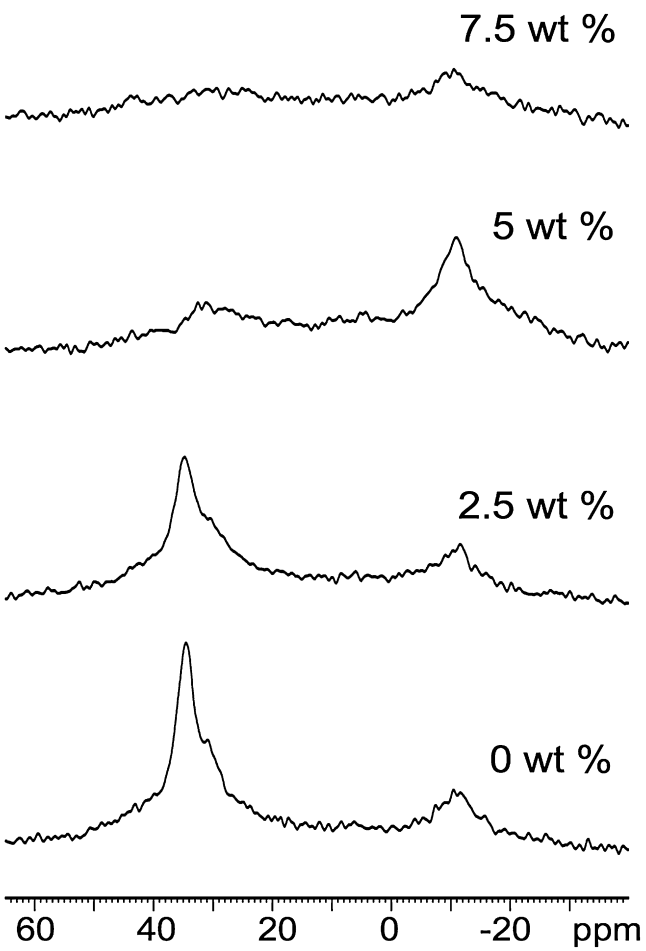

FIGURE 4 ^{31}P spectra (at $\mathbf{B_0}$ // $\mathbf{n}$) for BLES in the presence of increasing concentrations of SP-B_{CTERM}.

preferentially associate with DPPC over DPPG (57,58), presumably due to exclusion of the peptide from the more condensed DPPG domains. In this study, SP-B_{CTERM} certainly had a greater effect on pure POPG than pure POPC, as judged by loss of oriented material (as assessed by reductions in area under the $\sigma_{//}$ ^{31}P peak and increases in the ^{2}H spectral component with smaller splittings), by changes in headgroup orientation in both the oriented and unoriented fractions of the sample, and by increases in ^{2}H linewidth in POPG samples with peptide (Figs. 1 and 2). In 7:3 POPC/POPG, SP-B_{CTERM} appeared to preferentially affect the POPG component, as it was seen to induce greater area and chemical shift changes in the oriented ($\sigma_{//}$) PG peak compared to the PC peak in the ^{31}P spectra (Fig. 3 *b* and Fig. S2). A comparison with the single lipid results indicated that the presence of POPC in the lipid mixture reduced the effect of the peptide on POPG as compared to POPG alone, and vice versa. At 5% peptide, the degree of orientation disruption was comparable for POPG, POPC/POPG, and BLES, but at 2.5% peptide, BLES experienced more disruption than POPC/POPG. In contrast to the POPC/POPG model system, BLES contains ~45% saturated lipid chains and only ~10% anionic lipids, as well as SP-B, SP-C, and other lipid components (59). Thus, it appears that although headgroup charge is an important factor in determining the degree of disruption, other components present in BLES likely also modulate the peptide-induced disruption.

SP-B_{CTERM} is similar in overall topology to a large class of antimicrobial peptides with predominantly helical, amphipathic, cationic structure, which also function by mechanisms that involve disruption of bilayer structure. Full-length SP-B is member of the saposin superfamily, which contains several proteins with antimicrobial activities (60). Although full-length SP-B and peptide fragments of SP-B do display antimicrobial activity in laboratory assays for this characteristic, it is not thought to contribute to SP-B's in vivo role, since the antimicrobial activity is not specific for pathogenic membranes and is inhibited by surfactant lipids (61). Overall, the degree of peptide-induced orientation disruption observed for SP-B_{CTERM} was near the more severe end of the spectrum of disruption observed for helical antimicrobial peptides that have been studied with similar methods (52,62), as judged by the significant reduction of oriented species in the ^{31}P spectra.

As well as disrupting bilayer orientation, SP-B_{CTERM} also affects the configuration of the portion of the lipids in the sample that remain oriented, at least in the model lipid systems. This can be seen in the changes in the position of the $\sigma_{//}$ ^{31}P peak in the POPC, POPG, and POPC/POPG samples (Figs. 1 *b*, 2 *b*, 3 *b*, and Fig. S2), which indicate changes in headgroup conformation in the oriented portion of the sample. It should be emphasized that peptide-induced shifts in the $\sigma_{//}$ peaks of BLES were not observed, indicating that although SP-B_{CTERM} leads to levels of orientation disruption in BLES similar to those seen in the model systems, it does so without any apparent effect on lipid headgroup orientation.

The effect of the peptide on the oriented fraction of the model lipid samples is also seen in the reduction of quadrupole splittings of the oriented component of the ^{2}H spectra (Figs. 1 *a*, 2 *a*, and 3 *a*), which indicates a decreased acyl chain order of the oriented fraction of the samples in the presence of peptide. To quantify the effect of the peptide on chain order at different positions along the chain, order parameter profiles were extracted from the ^{2}H spectra (Fig. 5). For the POPC-d_{31} and POPC/POPG-d_{31} samples, it was possible to extract the order parameters using only the ^{2}H signals contributed by the oriented fraction of the sample, although due to the broader linewidths in the POPG-d_{31}/peptide spectra, the same analysis was not possible for those samples. The order parameter of the chains decreases with increasing peptide content, with the largest effects at approximately carbon 11 (see Fig. 5 and the fractional order parameter profiles in Fig. S3), indicating that the peptide affects acyl chain order deep within the bilayer. In the C10-C12 region of the order parameter profile, the peptide seems to have a greater effect on POPC-d_{31} than on the POPC/POPG-d_{31} mix (Fig. 5 and Fig. S3). This can potentially be explained if the peptide positions more deeply in the POPC/POPG bilayer and restricts chain motion, as opposed to a more peripheral interaction of the peptide with POPC, which would push the headgroups apart, allowing more freedom of motion for the acyl chains (63).

The order parameters in the plateau region (i.e., C2–6) are most indicative of lipid average area and were used to

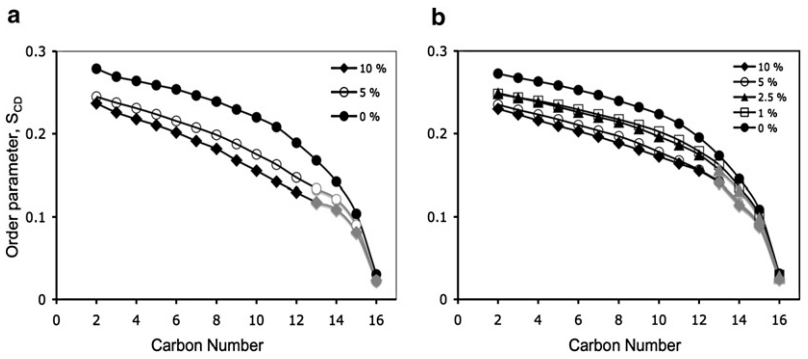

FIGURE 5 Order parameter profile, $|S_{CD}{}^{i}|$, of the *sn*1 chains of POPC-d_{31} (*a*), and POPG-d_{31} in POPC/POPG-d_{31} (= 7/3, w/w) (*b*) in the presence of increasing concentrations of SP-B_{CTERM}, as derived from Figs. 1 *a* and 3 *a*, respectively. The gray color of some of the markers indicates that these values were derived from clearly identifiable oriented peaks from ^{2}H spectral regions that were composed of superpositions of oriented and unoriented spectra.

calculate the average area, <A>, and thickness, D_C, of the saturated (*sn*1) acyl chain of the lipids using the mean torque method developed by Petrache et al. (48). In the absence of peptide, the average area per POPC-d_{31} lipid in POPC-only bilayers and that of POPG-d_{31} in POPC/POPG-d_{31} mixed bilayers was very similar (*a*). On the other hand, the area per lipid of POPG-d_{31} in POPG-only bilayers is significantly larger, as expected given the electrostatic repulsion between POPG headgroups. The addition of a small amount of peptide (1% w/w) led to a large change in the area per POPG-d_{31} lipid in POPC/POPG-d_{31}. At 5% peptide, the lipid area of POPC/POPG-d_{31} was ~1 $Å^2$ greater than in POPC-d_{31}, supporting the idea that electrostatic interactions lead to a greater impact of the peptide on the lipid area in anionic lipid-containing bilayers. At 10% peptide, the lipid area in POPC/POPG-d_{31} was only slightly higher than for POPC, which may indicate that this is close to the maximum area that both lipids can reach before their alignment is significantly disrupted. As the lipid acyl chains increase in area and experience more freedom of motion, there is a corresponding reduction in the thickness of the lipid chain area, as shown in Fig. 6 *b*.

SP-B_{CTERM} interacts with both the oriented and unoriented fraction of lipids in the samples, but it does not, in general, induce the same lipid conformation in both fractions. This result follows from comparing the ^{31}P and ^{2}H spectral features observed for the unoriented portion of the samples with what is predicted based on the oriented spectra (i.e., $\sigma_\perp = -\sigma_{//}/2$ for ^{31}P, and unoriented splittings = half oriented splittings for ^{2}H). Addition of peptide to pure POPC or pure POPG bilayers results in a relatively narrow ^{31}P $\sigma_\perp$ peak that does not follow well the expected scaling based on the position of the $\sigma_{//}$ peak, indicating that the conformation of the lipid headgroups is different in the oriented and unoriented fractions of the sample. Although the ^{2}H spectra match the expected scaling better, there does appear to be a discrepancy in the 10% peptide + POPG samples, indicating differences in the lipid acyl chain order in the oriented and unoriented fractions of this sample. In the POPC/POPG mix, the unoriented material displays a $\sigma_\perp$ peak close to the expected position at low peptide concentrations, but at high concentrations $\sigma_\perp$ deviates from the expectation even more than is seen in either POPC or POPG alone. The POPC/POPG $\sigma_\perp$ peak is also much broader than in either of the single lipid samples, indicating a broader range of lipid headgroup orientations. Notably, in BLES there is no apparent perturbation of lipid headgroup orientation by SP-B_{CTERM} on the oriented fraction of the lipids, and the unoriented fraction of the sample also conforms well to the expected ^{31}P chemical shift. In other words, SP-B_{CTERM} disrupts the orientation of the BLES bilayers without having any measurable impact on the headgroup conformation.

In comparison with earlier studies of full-length SP-B in DPPC or DPPC/DPPG vesicles (64–66), the effect of peptide SP-B_{CTERM} on lipids, including BLES, was much stronger in the study presented here, especially in terms of lipid order parameter, even though the concentrations of SP-B used in the earlier studies were much higher (up to 17 wt %) compared to the SP-B_{CTERM} in this study. The difference might be attributed to the effect of the N-terminal region of SP-B, i.e., the rest of the SP-B weakening the interaction with the lipids. However, the high degree of similarity in the ^{31}P spectra of BLES, which contains ~1% SP-B, and POPC/POPG, with 1% SP-B_{CTERM}, argues for a similarity in the lipid interactions of SP-B_{CTERM} and its parent protein, full-length SP-B. Alternatively, the source of the greater acyl chain parameter disruptions observed in this study may be explained by the differences in the levels of chain unsaturation present: in the earlier studies the chains were 100% saturated, whereas in this study they were either 100% asymmetric lipids with one unsaturated chain, as in the model lipid systems, or, in the case of the BLES study, still contained a significant fraction of unsaturated lipids (~55%) (41).

Lipid chain saturation is clearly a critical factor in modulating LS activity. In this study we used only unsaturated lipids in the model lipid systems, which allowed us to probe the effect of the lipid headgroups on the protein-bilayer interactions in the absence of chain saturation effects. However, although LS has a high unsaturated lipid content, the saturated lipid DPPC is clearly key in LS function (3,11). The ^{31}P spectra with BLES give an indication of how components of natural LS, especially DPPC and SP-C, modulate the effects of SP-B_{CTERM} on lipids. Although SP-B_{CTERM} had very similar effects on BLES and on the model POPG/

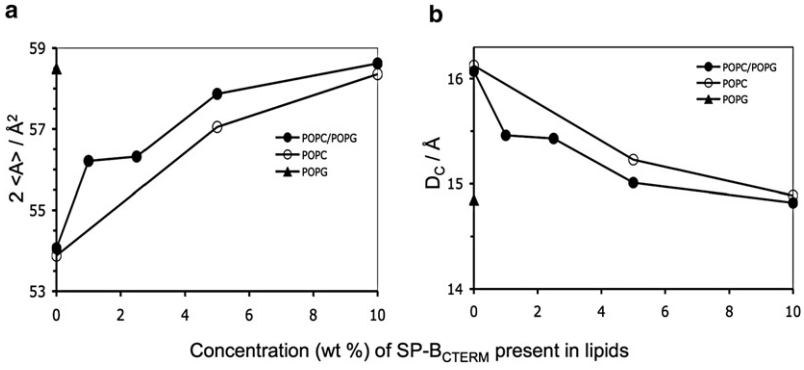

FIGURE 6 (*a*) Average area, <A>, of saturated (*sn*1) lipid acyl chains, and (*b*) D_C, average lipid hydrocarbon thickness per monolayer, of POPC-d_{31} and POPC/POPG-d_{31} as a function of SP-B_{CTERM} concentration. Because of the disruptive effect of the peptide on the spectra of POPG-d_{31} bilayers, only the data at 0% peptide are shown for the POPG-only samples.

POPC system in some respects (for example, on the degree of bilayer disruption), there was a major difference in the peptide's effects on the two systems in that the peptide perturbed lipid headgroup orientation in the model system but not in BLES. Further work is needed to elucidate the functional interactions present in natural LS, especially the effects of the saturated lipids, SP-C, and cholesterol, and to further probe the orientation and depth of SP-B_{CTERM} within the bilayers.

SUPPORTING MATERIAL

Three figures are available at http://www.biophysj.org/biophysj/supplemental/S0006-3495(09)00585-2.

The SP-B_{CTERM} used in this study was a gift from Alan Waring, and the BLES was a gift from BLES Biochemicals, Ontario, Canada. We thank Burkhard Bechinger and Philippe Bertani for performing preliminary studies with oriented SP-B_{CTERM}, and Dr. Celine Schneider for first-rate NMR technical support. We also acknowledge Donna Jackman for help in sample preparation.

This work was supported by grants from the Canadian Institutes of Health Research (to V.B.) and the Natural Sciences and Engineering Research Council of Canada (to M.R.M.).

REFERENCES

1. Clements, J. A. 1957. Surface tension of lung extracts. *Proc. Soc. Exp. Biol. Med.* 95:170–172.
2. Pattle, R. E. 1955. Properties, function and origin of the alveolar lining layer. *Nature.* 175:1125–1126.
3. Perez-Gil, J., and K. M. Keough. 1998. Interfacial properties of surfactant proteins. *Biochim. Biophys. Acta.* 1408:203–217.
4. Been, J. V., and L. J. Zimmermann. 2007. What's new in surfactant? A clinical view on recent developments in neonatology and paediatrics. *Eur. J. Pediatr.* 166:889–899.
5. Wright, J. R. 2005. Immunoregulatory functions of surfactant proteins. *Nat. Rev. Immunol.* 5:58–68.
6. Frerking, I., A. Günther, W. Seeger, and U. Pison. 2001. Pulmonary surfactant: functions, abnormalities and therapeutic options. *Intens. Care Med.* 27:1699–1717.
7. Kingma, P. S., and J. A. Whitsett. 2006. In defense of the lung: surfactant protein A and surfactant protein D. *Curr. Opin. Pharmacol.* 6: 277–283.
8. Pastva, A. M., J. R. Wright, and K. L. Williams. 2007. Immunomodulatory roles of surfactant proteins A and D: implications in lung disease. *Proc. Am. Thorac. Soc.* 4:252–257.
9. Serrano, A. G., and J. Pérez-Gil. 2006. Protein-lipid interactions and surface activity in the pulmonary surfactant system. *Chem Phys Lipids.* 141:105–118.
10. Goerke, J. 1998. Pulmonary surfactant: functions and molecular composition. *Biochim. Biophys. Acta.* 1408:79–89.
11. Zuo, Y., R. Veldhuizen, A. Neumann, N. Petersen, and F. Possmayer. 2008. Current perspectives in pulmonary surfactant—inhibition, enhancement and evaluation. *Biochim. Biophys. Acta.* 1778:1947–1977.
12. Revak, S. D., T. A. Merritt, E. Degryse, L. Stefani, M. Courtney, et al. 1988. Use of human surfactant low molecular weight apoproteins in the reconstitution of surfactant biologic activity. *J. Clin. Invest.* 81: 826–833.
13. Clark, J. C., S. E. Wert, C. J. Bachurski, M. T. Stahlman, B. R. Stripp, et al. 1995. Targeted disruption of the surfactant protein B gene disrupts surfactant homeostasis, causing respiratory failure in newborn mice. *Proc. Natl. Acad. Sci. USA.* 92:7794–7798.
14. Nogee, L. M., G. Garnier, H. C. Dietz, L. Singer, A. M. Murphy, et al. 1994. A mutation in the surfactant protein B gene responsible for fatal neonatal respiratory disease in multiple kindreds. *J. Clin. Invest.* 93:1860–1863.
15. Beck, D. C., M. Ikegami, C. L. Na, S. Zaltash, J. Johansson, et al. 2000. The role of homodimers in surfactant protein B function in vivo. *J. Biol. Chem.* 275:3365–3370.
16. Johansson, J., T. Curstedt, and H. Jornvall. 1991. Surfactant protein B: disulfide bridges, structural properties, and kringle similarities. *Biochemistry.* 30:6917–6921.
17. Andersson, M., T. Curstedt, H. Jornvall, and J. Johansson. 1995. An amphipathic helical motif common to tumourolytic polypeptide NK-lysin and pulmonary surfactant polypeptide SP-B. *FEBS Lett.* 362:328–332.
18. Vandenbussche, G., A. Clercx, M. Clercx, T. Curstedt, J. Johansson, et al. 1992. Secondary structure and orientation of the surfactant protein SP-B in a lipid environment. A Fourier transform infrared spectroscopy study. *Biochemistry.* 31:9169–9176.
19. Kurutz, J. W., and K. Y. C. Lee. 2002. NMR structure of lung surfactant peptide SP-B(11–25). *Biochemistry.* 41:9627–9636.
20. Booth, V. K., A. J. Waring, F. J. Walther, and K. M. W. Keough. 2004. NMR structures of the C-terminal segment of surfactant protein B in detergent micelles and hexafluoro-2-propanol. *Biochemistry.* 43: 15187–15194.
21. Sarker, M., A. J. Waring, F. J. Walther, K. M. W. Keough, and V. K. Booth. 2007. Structure of mini-B, a functional fragment of surfactant protein B, in detergent micelles. *Biochemistry.* 46:11047–11056.
22. Revak, S. D., T. A. Merritt, M. Hallman, G. Heldt, R. J. L. Polla, et al. 1991. The use of synthetic peptides in the formation of biophysically and biologically active pulmonary surfactants. *Pediatr. Res.* 29: 460–465.
23. Seurynck-Servoss, S. L., M. T. Dohm, and A. E. Barron. 2006. Effects of including an N-terminal insertion region and arginine-mimetic side chains in helical peptoid analogues of lung surfactant protein B. *Biochemistry.* 45:11809–11818.
24. Veldhuizen, E. J., A. J. Waring, F. J. Walther, J. J. Batenburg, L. M. van Golde, et al. 2000. Dimeric N-terminal segment of human surfactant protein B (dSP-B(1–25)) has enhanced surface properties compared to monomeric SP-B(1–25). *Biophys. J.* 79:377–384.
25. Walther, F. J., J. M. Hernandez-Juviel, L. M. Gordon, M. A. Sherman, and A. J. Waring. 2002. Dimeric surfactant protein B peptide sp-b(1–25) in neonatal and acute respiratory distress syndrome. *Exp. Lung Res.* 28:623–640.
26. Waring, A. J., F. J. Walther, L. M. Gordon, J. M. Hernandez-Juviel, T. Hong, et al. 2005. The role of charged amphipathic helices in the structure and function of surfactant protein B. *J. Pept. Res.* 66: 364–374.
27. Baatz, J. E., V. Sarin, D. R. Absolom, C. Baxter, and J. A. Whitsett. 1991. Effects of surfactant-associated protein SP-B synthetic analogs on the structure and surface activity of model membrane bilayers. *Chem. Phys. Lipids.* 60:163–178.
28. Longo, M. L., A. M. Bisagno, J. A. Zasadzinski, R. Bruni, and A. J. Waring. 1993. A function of lung surfactant protein SP-B. *Science.* 261:453–456.
29. Cochrane, C. G., and S. D. Revak. 1991. Pulmonary surfactant protein B (SP-B): structure-function relationships. *Science.* 254:566–568.
30. Cochrane, C. G., S. D. Revak, T. A. Merritt, G. P. Heldt, M. Hallman, et al. 1996. The efficacy and safety of KL4-surfactant in preterm infants with respiratory distress syndrome. *Am. J. Respir. Crit. Care Med.* 153:404–410.
31. Sinha, S. K., T. Lacaze-Masmonteil, A. Valls i Soler, T. E. Wiswell, J. Gadzinowski, et al. 2005. A multicenter, randomized, controlled trial of lucinactant versus poractant alfa among very premature infants at high risk for respiratory distress syndrome. *Pediatrics.* 115: 1030–1038.

32. Serrano, A. G., and J. Perez-Gil. 2006. Protein-lipid interactions and surface activity in the pulmonary surfactant system. *Chem. Phys. Lipids.* 141:105–118.

33. Blanco, O., and J. Perez-Gil. 2007. Biochemical and pharmacological differences between preparations of exogenous natural surfactant used to treat respiratory distress syndrome: role of the different components in an efficient pulmonary surfactant. *Eur. J. Pharmacol.* 568:1–15.

34. Klenz, U., M. Saleem, M. Meyer, and H. Galla. 2008. Influence of lipid saturation grade and head group charge: a refined lung surfactant adsorption model. *Biophys. J.* 95:699–709.

35. Cruz, A., L. Vázquez, M. Vélez, and J. Pérez-Gil. 2004. Effect of pulmonary surfactant protein SP-B on the micro- and nanostructure of phospholipid films. *Biophys J.* 86:308–320.

36. Nag, K., J. G. Munro, K. Inchley, S. Schürch, N. O. Petersen, et al. 1999. SP-B refining of pulmonary surfactant phospholipid films. *Am J Physiol.* 277:L1179–L1189.

37. Rodriguez-Capote, K., K. Nag, S. Schürch, and F. Possmayer. 2001. Surfactant protein interactions with neutral and acidic phospholipid films. *Am J Physiol Lung Cell Mol Physiol.* 281:L231–L242.

38. Morley, C. J., A. D. Bangham, N. Miller, and J. A. Davis. 1981. Dry artificial lung surfactant and its effect on very premature babies. *Lancet.* 1:64–68.

39. Morley, C. J., A. Greenough, N. G. Miller, A. D. Bangham, J. Pool, et al. 1988. Randomized trial of artificial surfactant (ALEC) given at birth to babies from 23 to 34 weeks gestation. *Early Hum. Dev.* 17:41–54.

40. Lang, C. J., A. D. Postle, S. Orgeig, F. Possmayer, W. Bernhard, et al. 2005. Dipalmitoylphosphatidylcholine is not the major surfactant phospholipid species in all mammals. *Am. J. Physiol. Regul. Integr. Comp. Physiol.* 289:R1426–R1439.

41. Yu, S., P. G. Harding, N. Smith, and F. Possmayer. 1983. Bovine pulmonary surfactant: chemical composition and physical properties. *Lipids.* 18:522–529.

42. Bligh, E. G., and W. J. Dyer. 1959. A rapid method of total lipid extraction and purification. *Can. J. Biochem. Physiol.* 37:911–917.

43. Fung, B. M., A. K. Khitrin, and K. Ermolaev. 2000. An improved broadband decoupling sequence for liquid crystals and solids. *J. Magn. Reson.* 142:97–101.

44. Rainey, J. K., and B. D. Sykes. 2005. Optimizing oriented planar-supported lipid samples for solid-state protein NMR. *Biophys. J.* 89:2792–2805.

45. Davis, J. H., K. R. Jeffrey, M. Bloom, M. Valic, and T. P. Higgs. 1976. Quadrupolar echo deueron magnetic resonance spectroscopy in ordered hydrocarbon chains. *Chem. Phys. Lett.* 42:390–394.

46. Sternin, E., B. Fine, M. Bloom, C. P. Tilcock, K. F. Wong, et al. 1988. Acyl chain orientational order in the hexagonal HII phase of phospholipid-water dispersions. *Biophys. J.* 54:689–694.

47. Burnett, L. J., and B. H. Muller. 1971. Deuteron quadrupole coupling constants in three solid deuterated paraffin hydrocarbons: C2D6, C4D10, C6D14. *J. Chem. Phys.* 55:5829–5831.

48. Petrache, H. I., S. W. Dodd, and M. F. Brown. 2000. Area per lipid and acyl length distributions in fluid phosphatidylcholines determined by (2)H NMR spectroscopy. *Biophys. J.* 79:3172–3192.

49. Seelig, J. 1978. 31P nuclear magnetic resonance and the head group structure of phospholipids in membranes. *Biochim. Biophys. Acta.* 515:105–140.

50. Balla, M. S., J. H. Bowie, and F. Separovic. 2004. Solid-state NMR study of antimicrobial peptides from Australian frogs in phospholipid membranes. *Eur. Biophys. J.* 33:109–116.

51. Ramamoorthy, A., S. Thennarasu, A. Tan, D. K. Lee, C. Clayberger, et al. 2006. Cell selectivity correlates with membrane-specific interactions: a case study on the antimicrobial peptide G15 derived from granulysin. *Biochim. Biophys. Acta.* 1758:154–163.

52. Hallock, K. J., D. Lee, and A. Ramamoorthy. 2003. MSI-78, an analogue of the magainin antimicrobial peptides, disrupts lipid bilayer structure via positive curvature strain. *Biophys. J.* 84:3052–3060.

53. Hyvonen, M. T., T. T. Rantala, and M. Ala-Korpela. 1997. Structure and dynamic properties of diunsaturated 1-palmitoyl-2-linoleoyl-sn-glycero-3-phosphatidylcholine lipid bilayer from molecular dynamics simulation. *Biophys. J.* 73:2907–2923.

54. Sachs, J. N., H. Nanda, H. I. Petrache, and T. B. Woolf. 2004. Changes in phosphatidylcholine headgroup tilt and water order induced by monovalent salts: molecular dynamics simulations. *Biophys. J.* 86:3772–3782.

55. Perez-Gil, J., C. Casals, and D. Marsh. 1995. Interactions of hydrophobic lung surfactant proteins SP-B and SP-C with dipalmitoylphosphatidylcholine and dipalmitoylphosphatidylglycerol bilayers studied by electron spin resonance spectroscopy. *Biochemistry.* 34:3964–3971.

56. Cruz, A., D. Marsh, and J. Perez-Gil. 1998. Rotational dynamics of spin-labelled surfactant-associated proteins SP-B and SP-C in dipalmitoylphosphatidylcholine and dipalmitoylphosphatidylglycerol bilayers. *Biochim. Biophys. Acta.* 1415:125–134.

57. Breitenstein, D., J. J. Batenburg, B. Hagenhoff, and H. Galla. 2006. Lipid specificity of surfactant protein B studied by time-of-flight secondary ion mass spectrometry. *Biophys. J.* 91:1347–1356.

58. Seifert, M., D. Breitenstein, U. Klenz, M. C. Meyer, and H. Galla. 2007. Solubility versus electrostatics: what determines lipid/protein interaction in lung surfactant. *Biophys. J.* 93:1192–1203.

59. Kang, N., Z. Policova, G. Bankian, M. L. Hair, Y. Y. Zuo, et al. 2008. Interaction between chitosan and bovine lung extract surfactants. *Biochim. Biophys. Acta.* 1778:291–302.

60. Munford, R. S., P. O. Sheppard, and P. J. O'Hara. 1995. Saposin-like proteins (SAPLIP) carry out diverse functions on a common backbone structure. *J. Lipid Res.* 36:1653–1663.

61. Ryan, M. A., H. T. Akinbi, A. G. Serrano, J. Perez-Gil, H. Wu, et al. 2006. Antimicrobial activity of native and synthetic surfactant protein B peptides. *J. Immunol.* 176:416–425.

62. Thennarasu, S., D. K. Lee, A. Tan, U. P. Kari, and A. Ramamoorthy. 2005. Antimicrobial activity and membrane selective interactions of a synthetic lipopeptide MSI-843. *Biochim. Biophys. Acta.* 1711:49–58.

63. Koenig, B. W., J. A. Ferretti, and K. Gawrisch. 1999. Site-specific deuterium order parameters and membrane-bound behavior of a peptide fragment from the intracellular domain of HIV-1 gp41. *Biochemistry.* 38:6327–6334.

64. Morrow, M. R., J. Perez-Gil, G. Simatos, C. Boland, J. Stewart, et al. 1993. Pulmonary surfactant-associated protein SP-B has little effect on acyl chains in dipalmitoylphosphatidylcholine dispersions. *Biochemistry.* 32:4397–4402.

65. Dico, A. S., J. Hancock, M. R. Morrow, J. Stewart, S. Harris, et al. 1997. Pulmonary surfactant protein SP-B interacts similarly with dipalmitoylphosphatidylglycerol and dipalmitoylphosphatidylcholine in phosphatidylcholine/phosphatidylglycerol mixtures. *Biochemistry.* 36:4172–4177.

66. Morrow, M. R., J. Stewart, S. Taneva, A. Dico, and K. M. W. Keough. 2004. Perturbation of DPPC bilayers by high concentrations of pulmonary surfactant protein SP-B. *Eur. Biophys. J.* 33:285–290.